Simulation of static operating modes of self-excited induction generator taking into account nonlinearity of the magnetic system

Mykola Pushkar[1,*,†], Nataliia Krasnoshapka[1,†], Hanna Zemlianukhina[1,†], Vasyl Budko[1,†], Aji Prasetya Wibawa[2,†] and Serhii Burian[1,†]

[1]National Technical University of Ukraine "Igor Sikorsky Kyiv Polytechnic Institute", Beresteiskyi Ave., 37, Kyiv, 03056, Ukraine
[2]State University of Malang, Jl. Cakrawala No.5, Sumbersari, Kec. Lowokwaru, Kota Malang, Jawa Timur, 65145, Indonesia

Abstract
The article deals with the issues of modeling static modes of autonomous generation systems with self-excited induction generator, taking into account the nonlinearity of the generator magnetization curve and with different load values. The simulation results, which have been verified experimentally, are presented and the three-dimensional dependences of frequency and amplitude of generated voltage, obtained by mathematical modeling, are given.

Keywords
induction generator, self-excitation, frequency and voltage control, generating system

1. Introduction

The use of autonomous power supply systems has become of great importance according the current state of the Ukrainian energy sector [1, 2]. Such systems are used as backup power sources or to provide electricity in the absence of centralized power supply. In such systems, in particular, self-excited induction generators (SEIG) are used. Asynchronous induction machines with a squirrel-cage rotor are characterized by small weight-and-dimensions and high reliability due to the absence of sliding contacts. One of the significant disadvantages of such technical solution is the complexity of the self-excitation process, which depends on many parameters - the generator rotation speed, the capacitance value and the connection scheme of self-excitation capacitors, as well as the load value [3]. An important aspect of the operation of autonomous power supply systems with SEIG is the stability of their operation when the load value changes [4]. To analyze static operating modes, mathematical modeling of the autonomous power supply system is carried out at different load values [5].

In [6] it is shown that the mathematical model of an induction generator with self-excitation must necessarily take into account the nonlinearity of the magnetization curve of the machine. The approach of piecewise linear approximation of the magnetization curve [7, 8] is widespread. This approach makes it impossible to obtain analytical dependencies that describe the operation of an induction generator, which, in turn, complicates the study of the entire generation system. In [9] an analytical description of the magnetization curve is proposed, which allows obtaining analytical dependencies for studying the operation of induction generator

Since the load of SEIG can vary during operation, the capacitance of the self-excitation capacitors is adjusted to stabilize the output voltage [10, 11].

CMSE'25: International Workshop on Computational Methods in Systems Engineering, June 12, 2025, Kyiv, Ukraine
*Corresponding author.
†These authors contributed equally.
pushkar.mykola@gmail.com (M. Pushkar); n.krasnoshapka@gmail.com (N. Krasnoshapka); annzemlya@gmail.com (H. Zemlianukhina); budko.vasyl@lll.kpi.ua (V. Budko); aji.prasetya.ft@um.ac.id (A. P. Wibawa); sburyan18@gmail.com (S. Burian)
https://epa.kpi.ua/department/staff/pushkar/ (M. Pushkar)
0000-0002-9576-6433 (M. Pushkar); 0000-0002-5449-2691 (N. Krasnoshapka); 0000-0002-9653-8416 (H. Zemlianukhina); 0000-0002-6219-4221 (V. Budko); 0000-0002-6653-2697 (A. P. Wibawa); 0000-0002-4947-0201 (S. Burian)

The purpose of this paper is to simulate the static operating modes of an autonomous generation system with a self-excited induction generator, taking into account the nonlinearity of magnetization curve depending on the magnitude of the applied load and to establish the relationship between the frequency and amplitude of the generated voltage and the generator load and the capacitor bank capacity, which will be useful for the development of generator voltage regulation systems.

2. Method

Let us consider the circuit of an induction generator when connecting self-excitation capacitors in a "triangle". We will consider the load to be active, because taking into account the inductive component leads to the need to solve sixth-order equations, which significantly complicates the obtaining of analytical dependencies [12]. Then the equivalent circuit will take the form (Figure. 1), where RL is the value of active resistance of the load in one phase:

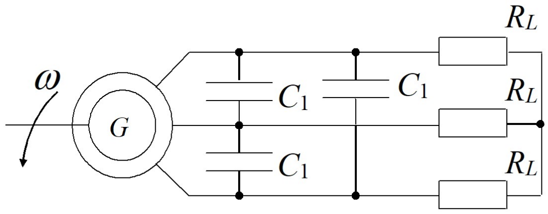

Figure 1: Equivalent circuit of SEIG.

When capacitors are connected in delta configuration, the total capacitance of the battery can be considered equal to C=3C1. The standard mathematical model of an induction generator in the rotating d–q coordinate system is described by the following nonlinear differential equations [11].

$$\begin{aligned} \frac{d\boldsymbol{\Psi_S}}{dt} &= \boldsymbol{U_S} - \boldsymbol{R_S i_S} - \omega_c \boldsymbol{J \Psi_S}, \\ \frac{d\boldsymbol{\Psi_R}}{dt} &= -R_R \boldsymbol{i_R} + (n_p\omega - \omega_c)\, \boldsymbol{J \Psi_R},\ \boldsymbol{J} = \begin{bmatrix} 0 & -1 \\ 1 & 0 \end{bmatrix}, \end{aligned} \tag{1}$$

where $\boldsymbol{\Psi_S} = \begin{bmatrix} \Psi_{Sd} & \Psi_{Sq} \end{bmatrix}^T$, $\boldsymbol{\Psi_R} = \begin{bmatrix} \Psi_{Rd} & \Psi_{Rq} \end{bmatrix}^T$ are vectors of stator and rotor fluxes in d-q coordinate system, $\boldsymbol{I_S} = \begin{bmatrix} I_{Sd} & I_{Sq} \end{bmatrix}^T$, $\boldsymbol{I_R} = \begin{bmatrix} I_{Rd} & I_{Rq} \end{bmatrix}^T$ are stator and rotor current vectors, $\boldsymbol{U_S} = \begin{bmatrix} U_{Sd} & U_{Sq} \end{bmatrix}^T$ is stator voltage vector in the coordinate system d–q, R_S and R_R are active resistances of the stator and rotor, n_p is a number of pole pairs; ω is an angular velocity of the induction generator rotor; ω_c is an angular velocity of an arbitrary coordinate system d–q.

Let us consider the equivalent circuit of one phase of a stand-alone generation system (Figure 2) According to Kirchhoff's current law, we can write that

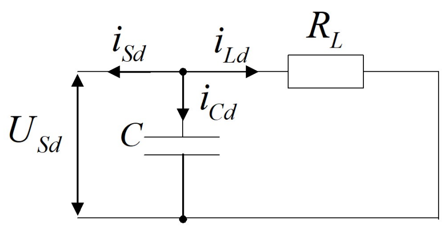

Figure 2: Phase equivalent circuit of the generation system.

$$\boldsymbol{i_S} + \boldsymbol{i_C} + \boldsymbol{i_L} = 0, \tag{2}$$

where $\boldsymbol{i_C} = \begin{bmatrix} I_{Cd} & I_{Cq} \end{bmatrix}^T$ and $\boldsymbol{i_L} = \begin{bmatrix} I_{Ld} & I_{Lq} \end{bmatrix}^T$ are urrent vectors in the coordinate system d–q.

As it is well known [11], [12] $\boldsymbol{i_C} = C\dfrac{d\boldsymbol{U_s}}{dt}$, thus, equation (2) can be represented as follows

$$-C\frac{d\boldsymbol{U_s}}{dt} = \boldsymbol{i_S} + \boldsymbol{i_L}. \tag{3}$$

The operation of a stand-alone generation system can be either stable or unstable. The stability region of steady-state modes depends on several factors [12]. In works [11, 12], an expression for the amplitude of the generated voltage at the equilibrium point has been derived.

$$|U_S^*| = \frac{\omega_c^* L_M^* i_M^*}{\sqrt{\left(1 + \frac{R_S}{R_L} - C\omega_c^{*2} L_{\sigma s}\right)^2 + \omega_c^{*2}\left(\frac{L_{\sigma s}}{R_L} + cR_S\right)^2}} \tag{4}$$

where $L_{\sigma s}$ is stator leakage inductance, L_M^* is magnetizing inductance, i_M^* is magnetizing current of induction generator. The symbol * will denote that the corresponding vector or variable is defined at the equilibrium point of the stand-alone generation system.

Another parameter of the steady-state operation mode of induction generator is generated voltage frequency. According to [11], its value is defined as

$$f_c^* = \frac{C - i_S - \dfrac{U_s}{R_L}}{2\pi C U_s} \tag{5}$$

where $f^* = \omega_c^*/2\pi$.

3. Approximation of magnetic curve

When the load of the generator or other parameters of the generation system change, the currents in the asynchronous machine, including the magnetizing current, also change [13]. This, in turn, leads to a change in the magnetizing inductance. Therefore, for each operating point in the steady-state mode, it is necessary to know the dependency $L_M = f(i_M)$. This dependency is not provided in the datasheets of asynchronous machines. The most common method for determining it is by experimentally obtaining the no-load characteristic of the asynchronous machine, and then deriving the dependency $L_M = f(i_M)$. based on it. However, this approach requires significant time and financial resources, as it necessitates a controllable voltage supply for the asynchronous machine. In [14], a method was shown for extrapolating an existing analytical dependency $L_M = f(i_M)$ from asynchronous machines of a similar type but different power ratings. This approach significantly simplifies the modeling process of the operation modes of stand-alone generation systems. Therefore, we will use this method for modeling the steady-state operation modes of the SEIG.

A schematic representation of the dependency $L_M = f(i_M)$ obtained using the no-load characteristic of the machine, is shown in Figure 3 [14].

The magnetizing inductance as a function of the magnetizing current can be divided into three regions. In the first — ascending — section, the magnetizing inductance increases from the initial value L_{M0} to L_{MAX}. The inductance L_{MAX} corresponds to the linear, unsaturated part of the magnetization curve of the asynchronous machine. In this region, only an unstable state is possible, meaning that both voltage generation and voltage collapse may occur [14]. In the second region — up to the saturation zone of the magnetic system — the inductance remains constant at L_{MAX}. The third region corresponds to the saturation zone of the asynchronous machine, where the magnetizing inductance decreases — the descending part of the $L_M = f(i_M)$ curve.

In our study we will use on experimental dependence [12] of magnetizing inductance LM on the magnetizing current iM, obtained in the idle mode test of asynchronous machine 6343 with the following

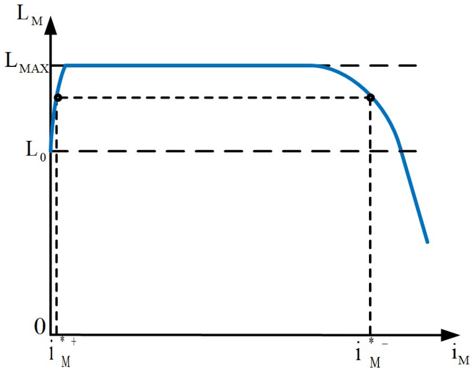

Figure 3: Dependency $L_M = f(i_M)$.

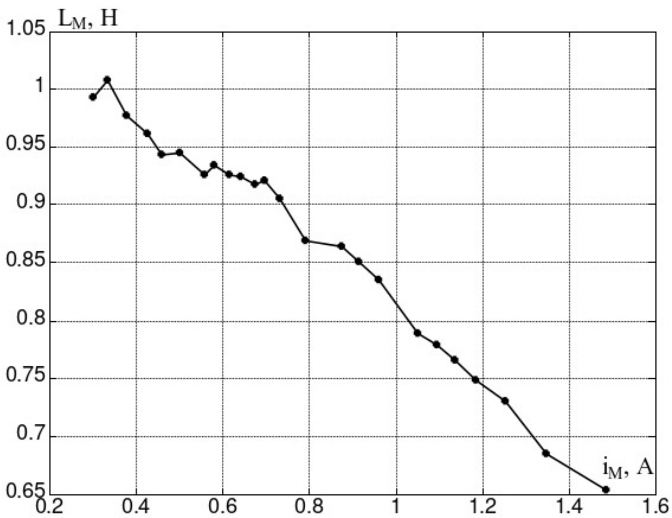

Figure 4: Experimental dependence $L_M = f(i_M)$.

nameplate data: rated power of 0.37 kW; Nominal stator phase voltage 220 V mains rated frequency 50 Hz, rated speed 1450 rpm, which is presented on Figure.4.

An important characteristics of SEIG are its self-excitation borders [9]. Moreover, the border of spontaneous self-excitation is determined at $i_M = 0$ and trigger self-excitation - in unsaturated linear section of the magnetization curve, which is characterized by the highest value LM [12]. Therefore, dependence $L_M = f(i_M)$ in Figure.3 have to be extrapolated, since the value $i_M = 0$.

Figure.5 shows the results of magnetizing inductance curve and dynamical inductance L approximation, described in [14]. Dependence $L_M = f(i_M)$ is presented in the form of four sections that are joined together without breaking the derivative.

In [14] was obtained that this approximation allows one to accurately describe the self-excitation border boundaries, which need to know primarily reliance $L_M = f(i_M)$ with small currents. However, as seen from Figure.5, in the steady-state operation modes a very significant deviation occurs between approximated and experimental dependencies, making this approach unacceptable to study these modes.

The descending part of the magnetization curve can be accurately described by polynomial equation of second order

$$L + M = p_1 i_M^2 + p_2 i_M + p_3. \tag{6}$$

Its factors may be determined using *polyfit* function in MATLAB. Figure.6 shows the results of magnetizing inductance L_M and dynamical inductance L approximation for values of approximation

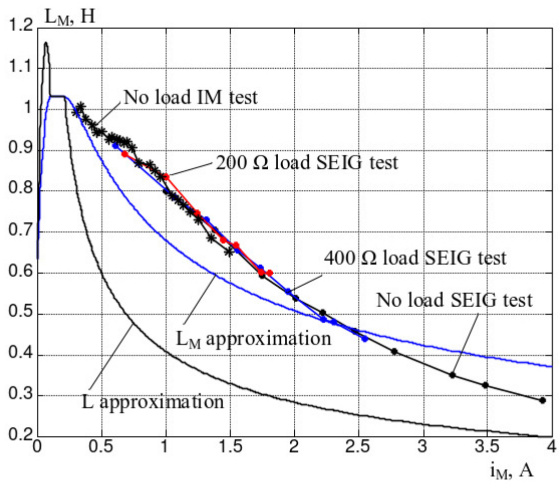

Figure 5: Magnetizing inductance curve and dynamical inductance approximation.

coefficients:

$$L = 3p_1 i_m^2 + 2p_2 i_M + p_3, \tag{7}$$
$$p_1 = 0.042433076890268;\ p_2 = \breve{}0.383816481755985;\ p_3 = 1.143841689235056,$$

which were obtained using MATLAB.

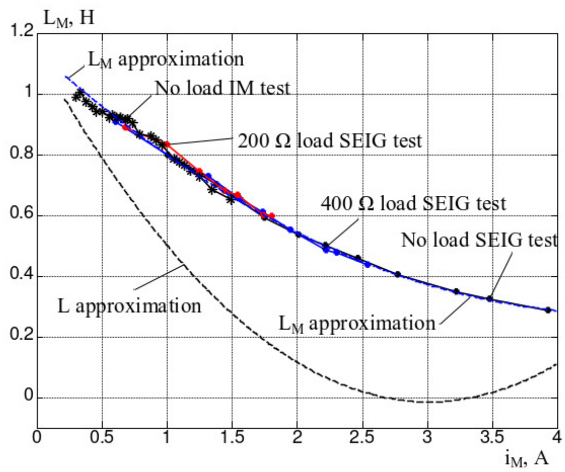

Figure 6: Results of approximation with polynomial equation of second order.

As seen from Figure.6, approximated magnetizing inductance accurately replicates the experimental curves on the descending part, and the dynamic inductance is negative and has growing part for large values of current, that is violating the physical nature of the phenomenon. Since in the study of steady-state of SEIG dynamic inductance is ignored, then this approach can be used in this case. But this approximation does not allow to consider the initial part of dependence $L_M = f(i_M)$ at low currents that will not allow its implementation for the study of boundary modes.

he inductance value is directly related to the dynamic inductance consider the magnetization curve approximation using dependence $\Psi_M = f(i_M)$. Dependencies $\Psi_M = f(i_M)$ that were obtained from experimental data of SEIG at mentioned above conditions for next values of the load 200 Ohm, 400 Ohm and no load case are depicted in Figure.7.

Approximation was performed by applying polyfit function in MATLAB to the saturated part of the flux linkage curve of SEIG for the case of no load. Points that are derived from the idle mode

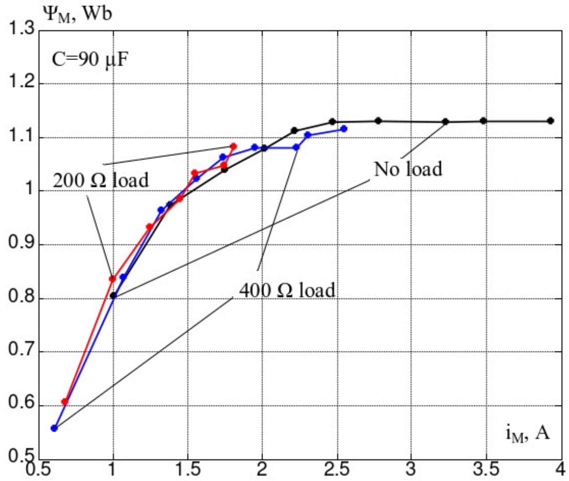

Figure 7: Experimental dependencies $\Psi_M = f(i_M)$.

characteristics of SEIG are marked with *, Figure.8.

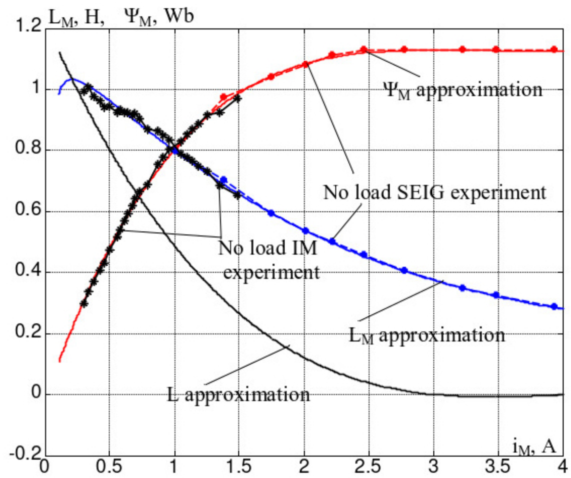

Figure 8: Results of approximation with polynomial equation of fourth order.

To account the unsaturated parts of magnetization curve the approximated dependence was amended with linear region in the left , that corresponds the inductance L_{MAX} at unsaturated part of magnetizing curve $(0,105 < i_M < 0,33\ )$, and "sewn" to it part without breaking the original of the initial magnetization $(i_M < 0,105\ )$. For the magnetizing currents $0,33 < i_M < 4$ flux linkage was approximated with fourth order polynomial equation:

$$\Psi_M = p_1 i_M^4 + p_2 i_M^3 + p_3 i_M^2 + p_4 i_M + p_5, \tag{8}$$

$$p_1 = \breve{\ }0.005214090677207;\ p_2 = 0.082454101449568;\ p_3 = \breve{\ }0.481133636330431;$$

$$p_4 = 1.225474520316153;\ p_5 = \breve{\ }0.020348151810052.$$

As shown in Figure.8, in the range of $0,105 < i_M < 0,33\ A$ magnetization inductance is not constant, equal L_{MAX}, and varies by a parabolic law. Therefore, in the area $i_M < 0,33\ A$ magnetizing inductance approximation was adjusted as follows: at the site of $0,105 < i_M < 0,33$ and $L_M = L = L_{MAX}$, it goes right in a downward part described with previously given fourth order polynomial equation. In addition, in the left it is described with a growing area of initial magnetization similarly as described in articles [6, 11].

To avoid the problems associated with negative values of dynamic inductance L when extrapolating on the high values of current i_M, the following correction was held. After the increase of magnetizing current, the dynamic inductance L first adopts zero, it is assumed that it must continue zero, and the value of flux Ψ_M also remains constant $\Psi_M = \Psi_{MMAX}$ (at $L = 0$). The results of this approximation are shown in Figure.9.

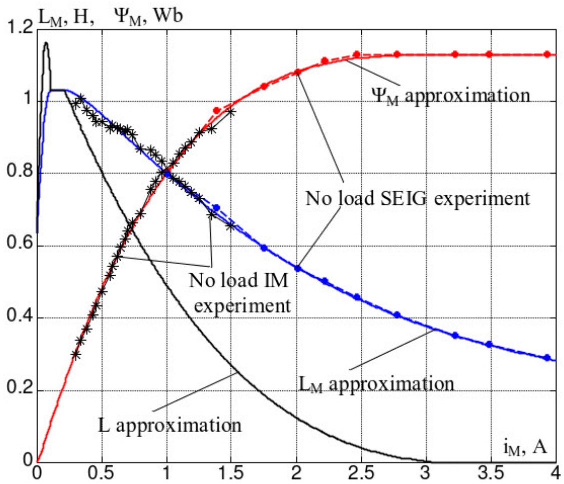

Figure 9: Results of approximation with correction for high current values.

Therefore, taking all the aforementioned factors into account, the magnetizing inductance of the asynchronous machine can be expressed through the following dependencies:

- at $i_M < i_{M1}$

$$L_M = L_{max} - b_1(i_M - i_{M1})^2, \tag{9}$$

  where b_1 – adjusted coefficient.
  Dynamic inductance is defined as:

$$L = L + MAX - b_1 i_{M1}^2 - b_1 i_M(3i_M - 4i_{M1}) \tag{10}$$

- at $i_{M1} < i_M < i_{M2}$

$$L = L_M = L_{MAX}. \tag{11}$$

  If the value of L_{M0} was obtained while $i_M = 0$, then coefficient b_1 will be determined by the ratio

$$b_1 = \frac{L_{MAX} - L_{M0}}{i_{M1}^2}. \tag{12}$$

- at $i_{M2} < i_M < i_{M3}$

$$\begin{gathered} L_M = p_1 i_M^4 + p_2 i_M^3 + p_3 i_M^2 + p_4 i_M + p_5; \\ L = 4p_1 i_M^3 + 3p_2 i_M^2 + 2p_3 i_M + p_4 \end{gathered} \tag{13}$$

- at $i_M > i_{M3}$

$$L_M = \frac{\Psi_{MMAX}}{i_M}, \; L = 0. \tag{14}$$

For the mentioned induction machine 6343 the next parameters of the approximation were accepted [12]:

$$\begin{gathered} L_{MAX} = 1.03115\ H;\ L_{M0} = 0.6345\ H;\ i_{M1} = 0.105\ A;\ i_{M2} = 0.2134 A; \\ i_{M3} = 3.042\ A;\ \Psi_{MMAX} = 1.129833270853887\ Wb; \\ p_1 = -0.005214090677207;\ p_2 = 0.082454101449568; \\ p_3 = -0.481133636330431;\ p_4 = 1.225474520316153; \\ p_5 = -0.020348151810052. \end{gathered} \tag{15}$$

4. Results

Thus, using equations (4) and (5), and taking into account the nonlinear dependence $L_M = f(i_M)$, the modeling of steady-state characteristics by using MatLab software's numerical routines and packages was performed, and the dependencies of the amplitude and frequency of the asynchronous generator voltage were obtained for two values of active load (Figure 10 and Figure 11) — 400 Ohms and 200 Ohms — as well as for the no-load condition. The calculations were carried out assuming a self-excitation capacitor bank capacitance of 90 Ohms, with varying generator shaft rotational speed.

The results obtained from modeling the steady-state modes were compared with experimental data acquired for the induction generator A634U3. The rated parameters of the machine are: power — 0.37 kW; stator phase voltage — 220 V; supply frequency — 50 Hz; rotational speed — 1450 rpm. As can be seen from the presented graphs, the modeling results are consistent with the experimental characteristics.

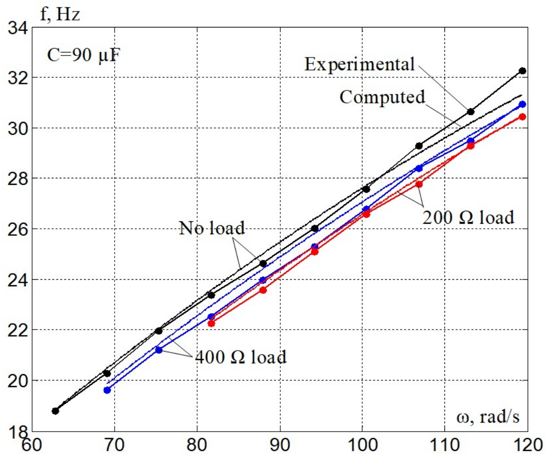

Figure 10: Dependency of frequency of SEIG voltage on angular velocity.

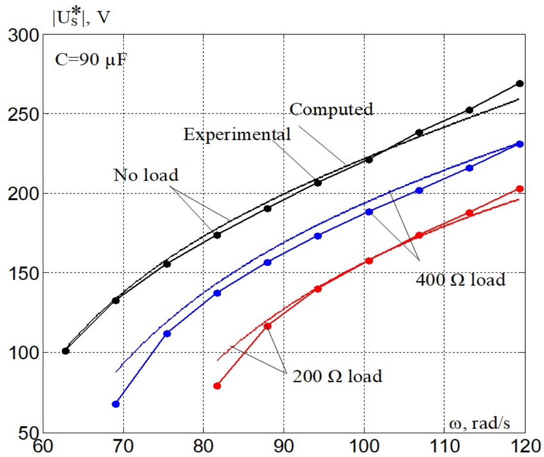

Figure 11: Dependency of amplitude of SEIG voltage on angular velocity.

The voltage and frequency values of the induction generator depend on three parameters: the load value, the capacitance of the self-excitation capacitor bank, and the generator shaft rotational speed [15]. To comprehensively assess the influence of these factors, we will model three-dimensional dependencies $f^*(C, 1/R_L)$ and $|U_S^*|(C, 1/R_L)$.

Figures 12 and 13 show the dependencies of the output voltage magnitude and frequency of the stand-alone generation system in steady-state operation mode, with varying load admittance $1/R_L$ within the self-excitation limits, at a generator shaft speed of 119.32 rad/s. Lines 1 indicate the boundaries of the self-excitation zone of the generation system, while lines 3 represent the maximum values of the function within this zone. Curves 2 on both graphs represent the projections of the three-dimensional graph onto the plane $C - 1/R_L$.

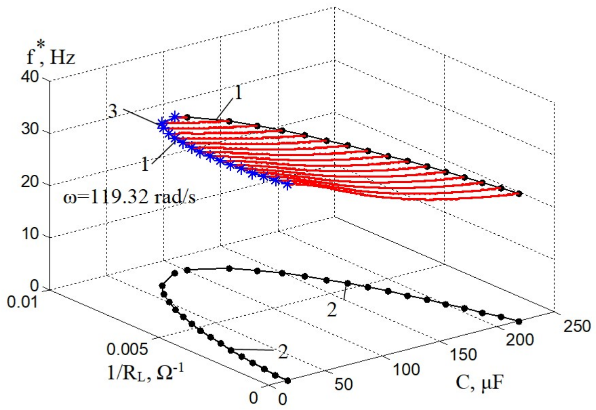

Figure 12: Steady-state dependences of the generated frequency on capacitance computed through the range of the load admittance.

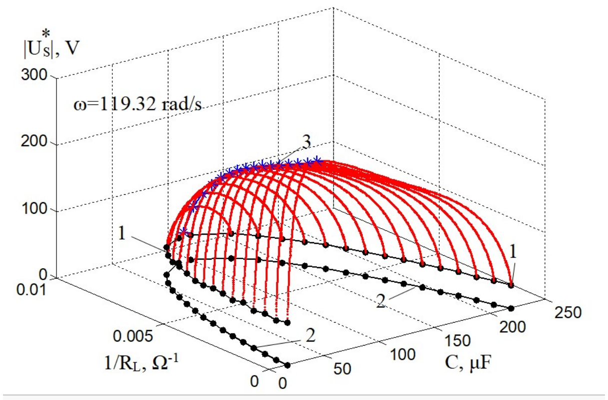

Figure 13: Steady-state dependences of the voltage magnitude on capacitance computed through the range of the load admittance.

Similarly, Figures 14 and 15 show the dependencies of voltage $|U_S^*|(C, 1/R_L)$ and frequency $f^*(C, 1/R_L)$ and with varying capacitance of the self-excitation capacitor bank within the self-excitation limits, at a generator shaft speed of 119.32 rad/s.

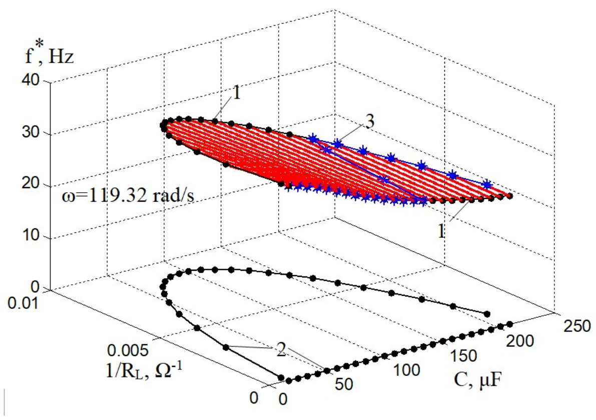

Figure 14: Steady-state dependences of the generated frequency on the load admittance computed through the range of capacitance.

A detailed analysis of the obtained graphs reveals that the maximum values of both frequency and

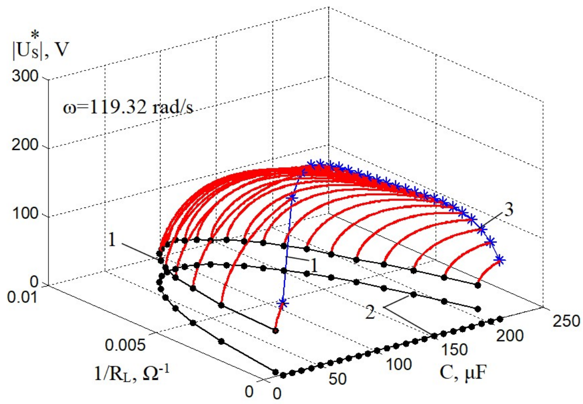

Figure 15: Steady-state dependences of the voltage magnitude on the load admittance computed through the range of capacitance.

voltage occur under no-load conditions. This is consistent with the physical behavior of SEIG [16], where the absence of load minimizes voltage drop and reactive power consumption, allowing the system to reach its peak performance. Furthermore, in both cases examined, the three-dimensional plots of the output voltage magnitude demonstrate pronounced maxima located near the center of the self-excitation boundary region. This indicates that the optimal operating point, in terms of voltage stability, lies within this central zone rather than at the extreme boundaries, which may be associated with unstable excitation conditions. These findings underscore the importance of carefully selecting system parameters to ensure operation within this optimal excitation region.

5. Conclusions

In this paper, the steady-state operating modes of a stand-alone generation system with an induction generator were modeled. The investigation was carried out with consideration of an analytical representation of the magnetization curve of the induction generator, which made it possible to derive analytical dependencies for the generator's voltage magnitude and frequency. A comparison between the modeling results and experimental data demonstrated a high level of agreement, thereby validating the accuracy of the proposed model.

Based on the developed models, three-dimensional plots were also obtained to analyze the combined influence of the self-excitation capacitor bank capacitance and load variation within the self-excitation limits of the induction generator, while maintaining a constant generator shaft speed. The analysis showed that the maximum values of the investigated quantities occurred under no-load conditions at the output of the stand-alone generation system.

Declaration on Generative AI

The author(s) have not employed any Generative AI tools.

References

[1] I. Trunina, K. Pryakhina, S. Yakymets, Research on the development of renewable energy sources in the world due to the war in Ukraine, in: 2022 IEEE 4th International Conference on Modern Electrical and Energy System (MEES), 2022, pp. 1–5. doi:10.1109/MEES58014.2022.10005696.

[2] R. Voliansky, V. Kuznetsov, A. Pranolo, Y. A. Fatimah, I. Amri, O. Sinkevych, Sliding mode control for DC generator with uncertain load, in: 2020 IEEE 15th International Conference on Advanced

Trends in Radioelectronics, Telecommunications and Computer Engineering (TCSET), 2020, pp. 313–316. doi:10.1109/TCSET49122.2020.235446.

[3] S. Chakraborty, R. Pudur, Performance study of a three-phase seig feeding single-phase non-linear loads, in: 2024 IEEE International Conference on Power Electronics, Drives and Energy Systems (PEDES), 2024, pp. 1–5. doi:10.1109/PEDES61459.2024.10961520.

[4] M. Bodson, O. Kiselychnyk, Nonlinear dynamic model and stability analysis of self-excited induction generators, in: Proceedings of the 2011 American Control Conference, 2011, pp. 4574–4579. doi:10.1109/ACC.2011.5991253.

[5] R. Voliansky, A. Pranolo, Parallel mathematical models of dynamic objects, International Journal of Advances in Intelligent Informatics 4 (2018) 120–131. doi:10.26555/ijain.v4i2.229.

[6] M. Bodson, O. Kiselychnyk, Analysis of triggered self-excitation in induction generators and experimental validation, IEEE Transactions on Energy Conversion 27 (2012) 238–249. doi:10.1109/TEC.2012.2182999.

[7] M. MROUEH, E. FRAPPE, A.-K. JIBAI, Hybrid identification method of magnetic saturation in an asynchronous motor, in: 2023 IEEE 8th Southern Power Electronics Conference and 17th Brazilian Power Electronics Conference (SPEC/COBEP), 2023, pp. 1–8. doi:10.1109/SPEC56436.2023.10408486.

[8] R. Volianskyi, O. Sadovoi, N. Volianska, O. Sinkevych, Construction of parallel piecewise-linear interval models for nonlinear dynamical objects, in: 2019 9th International Conference on Advanced Computer Information Technologies (ACIT), 2019, pp. 97–100. doi:10.1109/ACITT.2019.8779945.

[9] M. Pushkar, N. Krasnoshapka, M. Pechenik, S. Burian, H. Zemlianukhina, Approximation of magnetizing inductance curve of self-exited induction generator for investigation of steady-state operation modes, in: 2020 IEEE 7th International Conference on Energy Smart Systems (ESS), 2020, pp. 301–305. doi:10.1109/ESS50319.2020.9160143.

[10] A. k. Swain, S. k. Senapati, An experimental investigation of self-excitation in stand-alone induction generator, in: 2014 International Conference on Circuits, Power and Computing Technologies [ICCPCT-2014], 2014, pp. 245–249. doi:10.1109/ICCPCT.2014.7054906.

[11] O. Kiselychnyk, M. Bodson, J. Wang, Model of a self-excited induction generator for the design of capacitor-controlled voltage regulators, in: 21st Mediterranean Conference on Control and Automation, 2013, pp. 149–154. doi:10.1109/MED.2013.6608713.

[12] O. Kiselychnyk, J. Wang, M. Bodson, M. Pushkar, Steady-state and dynamic characteristics of self-excited induction generators with resistive-inductive loads, in: 2014 International Symposium on Power Electronics, Electrical Drives, Automation and Motion, 2014, pp. 625–630. doi:10.1109/SPEEDAM.2014.6871924.

[13] G. Nel, W. Doorsamy, Development of an intelligent electronic load controller for stand-alone micro-hydropower systems, in: 2018 IEEE PES/IAS PowerAfrica, 2018, pp. 366–371. doi:10.1109/PowerAfrica.2018.8521133.

[14] M. Pushkar, N. Krasnoshapka, M. Pechenik, D. Goloveshkin, V. Kypychrenko, Stability of operating modes of autonomous self-excited induction generators, Tekhn. Elektrodyn 3 (2024) 47–53. doi:10.15407/techned2024.03.047.

[15] B. T. Zine-Eddine, N. Ali, M. Said, I. Rachid, A balancing method for three-phase SEIG feeding a single-phase load by using switched capacitors, in: 2018 International Conference on Electrical Sciences and Technologies in Maghreb (CISTEM), 2018, pp. 1–6. doi:10.1109/CISTEM.2018.8613410.

[16] K. Teng, Z. Lu, J. Long, Y. Wang, A. P. Roskilly, Voltage build-up analysis of self-excited induction generator with multi-timescale reduced-order model, IEEE Access 7 (2019) 48003–48012. doi:10.1109/ACCESS.2019.2902977.